




Research Article

Binary Ethosomal Gel for Enhanced Transdermal Delivery of Tazarotene: Development, Refinement, *in vitro* Evaluation, and Skin Penetration Investigations

Mohammed Nihad Saadallah¹ , Yasir Qasim Almajidi^{2*} , Asgar Ali¹ 

¹ Department of Pharmaceutics, School of Pharmaceutical Education and Research, Jamia Hamdard, New Delhi 110062, India; ² Department of Pharmacy, Baghdad College of Medical Sciences, Baghdad 10011, Iraq

Received: 8 September 2023; Revised: 9 October 2023; Accepted: 15 October 2023

Abstract

Background: Tazarotene (TZ) is a novel acetylenic class retinoid that selectively targets RAR β/γ . It is not particularly soluble or bioavailable, yet it is used to treat melanoma. **Objective:** To improve the tazarotene gel formula's transdermal distribution. **Methods:** TZ-incorporated binary ethosomes (TZ-BES) were developed for the current study. The cold technique and optimized Box-Behnken statistical design tools were used to synthesize the TZ-BES. The improved ethosome (TZ-BES13) was mixed with carbopol gel and tested for stability and *ex vivo* skin penetration, as well as viscosity, pH, spreadability, and drug content. **Results:** The optimal ethosomes (TZ-BES13) had a vesicle size of 168 nm, a PDI of 0.367, a zeta potential of -30 mV, and an entrapment effectiveness of 79.94%. TZ is enclosed in the ethosome matrix, as seen by the differential scanning calorimetry thermogram. FTIR shows that the TZ and additives are compatible. TZ-BES13-G2, the optimized TZ-BES13 gel, has a spreadability of 7.82 cm², a pH of 6.52, a viscosity of 17235, and a drug content of 99.82 \pm 1.04%. Compared to the plan TZ-gel (43.54%), the TZ-BES13-G2 exhibits a much higher TZ release (89.22%). In 6 hours, rat abdomen skin permeability for TZ-BES13-G2 was 66.22 \pm 3.31%, much greater than that of plan TZ-gel (24.67%). The flow of TZ-BES13-G2 was 2.68 times greater than that of plan TZ-gel. The stability analysis showed that the formulation's properties had not changed significantly. **Conclusion:** Ethosomal gel offers an alternative mode of TZ administration when used topically.

Keywords: Binary ethosomes, 3² Full factorial design, Melanoma, Tazarotene, Transdermal drug delivery.

جل إيثنوزومي ثنائي لتعزيز توصيل التازاروتين عبر الجلد: التطوير والصقل والتقييم في المختبر ودراسات اختراق الجلد

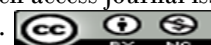
الخلاصة

الخلفية: تازاروتين هو عضو جديد في فئة الأسيثيلين من الريتينويدات الانتقائية لعلاج سرطان الجلد مع قابلية ذوبان وتوافر حيوي محدودة. **الهدف:** تحسين توزيع تركيبة هلام التازاروتين عبر الجلد. **الطرق:** في التحقيق الحالي، تم إعداد الاثوسومات الثنائية للتغلب على هذه المزالق. تم تصنيع الاثوسومات الثنائية بالطريقة الباردة وتحسينها باستخدام برنامج التصميم الإحصائي المحسن. تم دمج الإيثوسومات المحسنة في جل كاربول وتم تقييمها من حيث اللزوجة، ودرجة الحموضة، وقابلية الانتشار، ومحتوى الدواء، وإطلاق الدواء، ودراسة نفاذ واستقرار الجلد خارج الجسم الحي. **النتائج:** تمتلك الإيثوسومات المحسنة حجم حويصلة يبلغ 168 نانومتر، وكفاءة انحباس تبلغ 79.94%، ومعدل انتشار متعدد تبلغ 0.367، وإمكانات زيتا تبلغ -30 مللي فولت. يُظهر الرسم الحراري لقياس السرعات الحرارية بالمسح التفاضلي أن التازاروتين مغلف في مصفوفة الأيثوسومات. هناك توافق بين التازاروتين والمواد المضافة، كما يتضح في الأشعة تحت الحمراء. يتمتع جل التازاروتين الأمثل بلزوجة تبلغ 17235، ودرجة حموضة تبلغ 6.52، ومحتوى دوائي يبلغ 99.82%، وقابلية انتشار تبلغ 7.82 سم². يُظهر جل التازاروتين الأمثل تحرر تازاروتين عاليًا (89.2%) مقارنة بالجل الخالي (43.54%). أظهر جل التازاروتين الأمثل تخللاً أعلى بكثير (66.2%) عبر جلد البطن لدى الفئران مقارنة بالجل الخالي (24.67%) في 6 ساعات. أظهر جل التازاروتين الأمثل تدفقاً أعلى بمقدار 2.68 ضعفاً من الجل الخالي. أظهرت نتائج دراسة الاستقرار عدم وجود تغيير مهم في خصائص الصياغة. **الاستنتاج:** جل الإيثوسومال هو طريقة مختلفة لتوصيل التازاروتين عند تطبيقه موضعياً.

* **Corresponding author:** Yasir Q. Almajidi, Department of Pharmacy, Baghdad College of Medical Sciences, Baghdad 10011, Iraq; Email: yasir.qasim.mohammed@bcms.edu.iq

Article citation: Saadallah MN, Almajidi YQ, Asgar A. Binary ethosomal gel for enhanced transdermal delivery of tazarotene: Development, refinement, *in vitro* evaluation, and skin penetration investigations. *Al-Rafidain J Med Sci.* 2023;5(Suppl 1):S42-50. doi: <https://doi.org/10.54133/ajms.v5i1S.288>

© 2023 The Author(s). Published by Al-Rafidain University College. This is an open access journal issued under the CC BY-NC-SA 4.0 license (<https://creativecommons.org/licenses/by-nc-sa/4.0/>).



INTRODUCTION

Melanoma is a cancer that affects the melanocytes with the highest metastatic effect rate [1]. It can be propagated to a distant body region by invading the lymphatic system and bloodstream. Despite its early discovery, adequate surgical resection, and adjuvant chemotherapy, it may be the most malignant skin carcinoma [2]. Particularly in this aspect, tazarotene (TZ) is effective in preventing and managing melanoma. TZ is an exciting adherent of the acetylenic class of RAR β/γ selective retinoids and has been approved by the Food and Drug Administration (FDA) to cure various skin diseases [3]. Chemically, it is ethyl 6-[2-(4,4-dimethyl-3,4-dihydro-2H-1-benzothioopyran-6-yl) ethynyl] pyridine-3-carboxylate. It suppresses human melanoma cell proliferation by activating caspase-8/t-Bid and the reactive oxygen species-dependent mitochondrial pathway [4]. Melanoma may be effectively treated with topical application of TZ cream; however, expected adverse consequences include redness, burning, stinging, and peeling at the application site. TZ has low solubility and low bioavailability (14%) [5]. It has been reported that various vesicular delivery systems integrated into gel have improved transdermal distribution of poorly soluble drugs, i.e., itraconazole-loaded liposomes gel, and showed 2.99-fold higher skin permeation than conventional cream [6], fluconazole-loaded proniosomes gel, and significant high antifungal activity than plane gel [7], niosomes gel of luliconazole [8], cilostazole-loaded proniosomes gel, and improved skin permeation [9], ethosomal gel loaded with terbinafine hydrochloride [10], transferosomes loaded with Ivabradine HCl, and showed higher permeability and retention in rat skin than pure drug [11]. One creative carrier is ethosomes, which are made up of phosphatidylcholine, a lot of water, and ethanol (20–45% v/v) [12]. This high ethanol content made it much easier to shape, dissolve, stay stable, pass through, be bioavailable, and work as a therapeutic for poorly soluble therapeutics. Ethosomes' relatively high negative surface charge may increase their stability [13]. However, the high ethanol concentration may contribute to drug leakage outside the vesicle, resulting in low drug entrapment and penetration [14]. Hence, these systems are focused on the exploration of binary ethosomes (BES) comprising isopropyl alcohol and propylene glycol (binary alcoholic system) [15]. Soy-lecithin and alcohols improve drug permeability through the skin by disturbing the stratum corneum barrier of the skin layer through the transdermal drug delivery system [16]. Further incorporation of ethosome into a gel using gelling polymers can improve drug release and permeability and reduce side effects. The present study prepared the TZ-loaded BES-gel for increasing skin stability, permeability, and therapeutic effectiveness.

METHODS

Materials

Tazarotene was purchased from (TCI Chemicals Industries, Mumbai, India). The soya lecithin and cholesterol, Carbopol 934 P, Ethanol, Propylene glycol, and Isopropyl alcohol were procured from (Delta Chemicals, Mumbai, India).

Preparation of the formula

For the development of the binary ethosomes, the cold method was used to prepare binary ethosomes as described by Shukla and its associates [17]. The SL and CL were weighed and dissolved in ethanol (30 ml) under continuous mechanical stirring (1500 rpm, Remi Instruments Ltd., Mumbai, India). The mixture of the drug (1 mg/ml), propylene glycol, and isopropyl alcohol (5:5) (v/v) was added to the above lipid solution and warmed at 30°C in a water bath. The aqueous phase was gradually injected into the lipid phase in a fine stream with continuous stirring (700 rpm). After injection of all aqueous phases, the mixture continued to be stirred for 30 minutes for the stabilization of ethosomes. Finally, the ethosomal suspension was sonicated at a 30-second interval for 2–6 minutes. The TZ-BES formulation was cooled at room temperature and stored at 4–8 °C for further assessment [18].

Optimization of Ethosomes

Experimental design software (Design-Expert® Version-7, Stat Ease Inc., Minneapolis, MN, USA) optimized the TZ-ES. A 3-level and 3-factor Box-Bhekhen design was applied for optimization. Soy-lecithin (SL), cholesterol (CL), and sonication time are the independent variables, and vesicle (VS) and entrapment efficiency (EE%) were selected as the dependent variables. The thirteen formulations of different compositions were found in the software. To select the best-fit model, the VS and EE results of each formulation were fitted into several design models. Both fitted models for the responses were subjected to an analysis of variance (ANOVA). The software was used to create the response surface plot (3D), which depicts the effect variables on the response.

Vesicle size polydispersity index and zeta potential

The VS, PDI, and zeta potential of the TZ-BES formulation were analyzed by the Malvern nano zeta-sizer. The diluted sample was put into a quartz cuvette for the tenth time before being examined for 180 seconds at 25 °C with a 90° scattering angle [19]. The zeta potential was measured by using a zeta potential electrode cuvette.

Entrapment efficiency (% EE) and drug loading

The percent EE and drug loading evaluated the amount of drug encapsulated inside the developed vesicles. The concentration of TZ in the BES was

assessed by ultracentrifuging of TZ-BES (Bachman Coulter USA) at 12,000 rpm for 30 min. The clear supernatant was separated, and absorbance was determined by UV-spectrophotometric absorbance (UV 1700, Shimadzu, Japan) at 351 nm. The following equation was used for calculating the drug loading of TZ and the percent EE (1, 2) [20].

$$\%EE = \frac{\text{Amount of TZ added} - \text{Amount of TZ in supernatant}}{\text{Amount of drug added}} \times 100 \quad (1)$$

$$\% \text{ Drug loading} = \frac{\text{Amount of TZ added} - \text{amount of TZ supernates}}{\text{weight of BE}} \times 100 \quad (2)$$

Transmission electron microscopy

The optimized TZ-ES formulation was dropped over the formvar-coated 300 mesh grids for one minute and air-dried. The excess amount was soaked with filter paper. Then it was stained with 2% phosphotungstic acid, and the excess volume was soaked with filter paper. The grid was placed in a sample holder and put into a TEM instrument (JEOL 100CX, Tokyo, Japan) operated at 80 kV, which captured the image [21].

Fourier-Transform Infrared spectroscopy study

FTIR was employed to ascertain the compatibility between TZ and additives in the TZ-BES formulation. The FTIR study of TZ, physical mixture, and TZ-BES (3 mg) was done by an FTIR instrument (FTIR-8400S,

Shimadzu, Japan). The spectra were captured and analyzed [22].

Thermal analysis

Thermal analysis of TZ, physical mixture, and TZ-BES was done by differential scanning calorimetry (DSC, Mettler Toledo Ltd., USA). For the calibration of the instrument, an indium standard was used. The (2 mg) sample was weighed precisely, packed, and placed in a DSC aluminum pan. The empty pan was utilized as a reference standard. The sample was scanned from 25 °C to 300 °C at a rate of 10 °C/min. The nitrogen gas was employed at a rate of 20 ml/min to provide the inner environment [23].

Development of TZ – BES gel

Using the gelling agent carbopol 934P, the optimized TZ-BES was converted into gel using the cold method. The composition of different batches is given in Table 1. The different concentrations of carbopol 934 P were dissolved in cold water with continuous stirring. The carbopol 934P gel was continuously stirred while the optimized TZ-BES (1% w/w) was incorporated. Simultaneously, propylene glycol and sodium methyl hydroxyl benzoate were added to the gel formulation and stored at 4 °C for extra evaluation [24]. For the comparative study, a plangel (TZ-gel) was created.

Table 1: Composition of various TB-BES formulations and results of responses (VS and %EE)

Std. order	Soy lecithin (A%)	Cholesterol (B%)	Sonication time (min)	Vesicle size (nm)	EE (%)
TZ-ES 1	1.5	2	4	73.23±4.62	63.64±1.43
TZ-ES 2	3	2	4	171.34±3.56	78.52±1.32
TZ-ES 3	1.5	4	4	143.6±4.03	82.14±1.01
TZ-ES 4	3	4	4	279.62±5.21	91.52±2.12
TZ-ES 5	1.5	3	2	105.72±6.43	77.23±1.32
TZ-ES 6	3	3	2	242.12±6.02	84.62±0.92
TZ-ES 7	1.5	3	6	116.71±4.63	69.02±1.05
TZ-ES 8	3	3	6	198.31±4.72	84.12±1.41
TZ-ES 9	2.25	2	2	130.11±3.51	75.81±1.56
TZ-ES 10	2.25	4	2	225.52±4.31	87.52±1.22
TZ-ES 11	2.25	2	6	118.92±5.03	66.92±1.74
TZ-ES 12	2.25	4	6	206.54±4.23	85.66±1.02
TZ-ES 13	2.25	3	4	168.00±3.62	79.94±1.43

Characterization of TZ -BES Gel

pH and viscosity analysis

A digital pH meter was used to determine the pH of the TZ-ES-loaded gel. An Ametex Brookfield RV viscometer was used to measure the viscosity of all TZ-BS-included gel at 25°C and 30 rpm [25].

Spreadability

The Petri dish method was used to gauge the spreadability of all TZ-ES gels. 0.5g of the gel was placed over the Petri dish, and the diameter was noted. The second Petri plate was placed over the gel and added; the weight was over for 5 minutes, and the

diameter was noted. The percentage spreadability was calculated [26].

In-vitro release study

The dialysis bag was used to conduct in-vitro release research on the optimized TZ-ES, TZ-ES Gel, and pure TZ. The treatment involved submerging the dialysis bag in distilled water for 12 hours. The dialysis bag was filled with the necessary amount of TZ-ES and TZ-ES Gel (equivalent = 2 mg), and both ends were securely tied. A beaker was filled with the releasing media (phosphate buffer, pH 6.8, 250 ml), and a thermostatic magnetic stirrer was used to keep the temperature at 37°C. The dialysis bag was submerged in a solution for dissolving, and at the

appointed time, 5 ml of the aliquot was removed and replaced with the same volume of fresh solution. A membrane filter was used to filter the aliquot, and the absorbance at 351 nm (0.22 m) was measured using UV-spectrophotometry. The percentage of drug release was computed, and a graph showing time vs. percentage of drug release was created [22]. To determine the best-fit model and drug release mechanism, the release profile of the TZ-BES Gel was fitted into various kinetic release models.

Ex-vivo permeation study

Using excised rat skin and the Franz diffusion method, ex-vivo permeation research was carried out. The animal study protocol was approved by the Iraqi Center for Cancer Research/Mustansiriyah University animal ethics committee (approval no. ICCMGR2020-016). The animal fasted overnight before starting the study. The abdominal skin and hairs of the sacrificed rat were taken without any damage and washed with 0.9% NaCl. The excised skin was fitted between the donor and acceptor compartments of the diffusion cell, and 15 ml of permeation media (phosphate buffer, pH 6.8) was filled into the acceptor compartment of the diffusion cell and maintained at $36 \pm 1^\circ\text{C}$ during the whole study. The specific time interval at the aliquot was withdrawn from the acceptor compartment, filtered with a $0.22 \mu\text{m}$ membrane filter, and the concentration was determined by the previously reported validated HPLC method [27]. The following equation was used to compute both the penetrated flux and apparent permeability co-efficiency (Papp).

$$J_{ss} = (Dq / dt) / A \text{ --- (3)}$$

$$P_{app} = J_{ss} / C_0 \text{ --- (4)}$$

Where: (Dq / dt) is the amount of TZ permeated ($\mu\text{g/h}$); A is the surface area of the used membrane (cm^2); C_0 is the initial TZ concentration.

Skin deposition study

The rat abdomen membranes were whipped with cotton dipped in phosphate buffer and then rinsed in the same solution three times after the permeation study. The membranes were divided into 16 pieces, placed in 10 mL of ethanol vials, and exposed to ultrasonication for 30 minutes (Analab Scientific Instruments Pvt. Ltd., India). The suspension was then filtered through $0.22 \mu\text{m}$ nylon syringe membranes, and this concentration of the drug was analyzed by the previously reported validated HPLC method. The percentage of TZ deposited into the membrane was calculated [22].

Accelerated stability study

The stability analysis of the improved formulation (TZ-BES13-G2) was carried out following the international harmonization conference Q1A (R2) (ICH, 2003). The gel was packaged in lacquer-coated tubes and kept in a stability chamber for three months at 4°C , 25°C with 65% relative humidity, and 30°C with 75% RH. Samples from the stability chamber were taken at regular times (0, 1, 2, and 3 months) and tested for viscosity, pH, and drug content analyses [10].

RESULTS AND DISCUSSION

Table 1 lists the components of each TZ-BES formulation as well as the responses' outcomes (VS size and entrapment efficiency). The response's relationship with the level of the formulation component was explained using a polynomial equation. The best model for particle size and entrapment effectiveness was the second-order model. For both models, the absence is not significant ($p > 0.05$). Data from the ANOVA analysis of the best-fitting model for both responses are shown in Table 2.

Table 2: ANOVA for best fitted 2FI Model for vesicle size and entrapment efficiency

Vesicle size						
Source	Sum of Squares	df	Mean Square	F value	p-value	
Model	43525.58	6	7254.263	530.32	< 0.0001	
A-Soyalecithin	25552.18	1	25552.18	1868.00	< 0.0001	
B-Cholesterol	16352.23	1	16352.23	1195.43	< 0.0001	
C-Sonication time	495.92	1	495.92	36.25	0.0009	
AB	359.30	1	359.30	26.26	0.0022	
AC	750.76	1	750.76	54.88	0.0003	
BC	15.18	1	15.182	1.11	0.3327	
Residual	82.07	6	13.67			
Cor Total	43607.65	12				
Entrapment efficiency						
Source	Sum of Squares	df	Mean Square	F value	p-value	
Model	835.06	6	139.17	382.11	< 0.0001	
A-Soyalecithin	272.97	1	272.97	749.44	< 0.0001	
B-Cholesterol	480.03	1	480.03	1317.93	< 0.0001	
C-Sonication time	47.34	1	47.34	129.97	< 0.0001	
AB	7.50	1	7.50	20.61	0.0039	
AC	14.85	1	14.85	40.79	0.0007	
BC	12.35	1	12.35	33.92	0.0011	
Residual	2.18	6	0.36	--	--	
Cor Total	837.25	12	--	--	--	

Figures 1 and 2 show the 3D plots for each answer, which indicate how the formulation variable affects the response. The polynomial equation for VS is below:

$$\text{Particle size (Y1)} = 167.53 + 56.51A + 45.21B - 7.87C + 9.47 AB - 13.71AC - 1.94 BC \quad \text{---(1)}$$

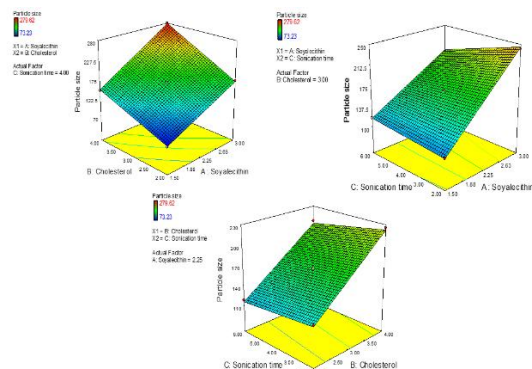


Figure 1: Response surface plots for the effect of SL, CL concentration and sonication on vesicle size of ethosomes.

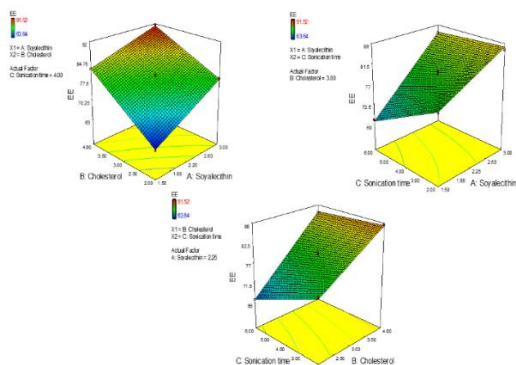


Figure 2: Response surface plots for the effect of SL, CL concentration, and sonication time on entrapment efficiency TZ in ethosomes.

Here the equation shows the significant model term, which significantly ($p < 0.05$) affects the particle size. A, B, C, AB, and AC are the significant model terms ($p < 0.05$), and BC is an insignificant model term ($p = 0.33$). The second-order model is the best fit for particle size because it has a higher R^2 (0.9981) than another experimental model. The predicted R^2 of 0.9897 is in reasonable agreement with the "adjusted R^2 of 0.9962. A model F-value of 530 implies that terms with $p < 0.05$ are considered significant. The adequate precision is 74.96, indicating a satisfactory signal. The ANOVA of the fitted model was evaluated, and the data are shown in Table 2. The 3D and contour plots of particle size determined the effect of independent variables (Figure 1). The particle size of all TZ-BES was found in a range of 73.23 ± 4.62 (TZ-ES1) to 279.62 ± 5.21 (TZ-ES4) (Table 1). The 3D plot and polynomial equation showed that particle size considerably increases with an increase in the concentrations of SL (1.5–3% w/w) and CL (2–4% w/w). It is due to the deposition of CL on the surface of ES, which increases the viscosity of the solution with increasing SL. These results agreed with the

previous finding. However, sonication time increases the VS. However, with the increase in sonication time, the particle size of ES decreases because of the breaking of the particle during sonication [28]. The polynomial equation of the fitted second-order model for EE is shown below:

$$\text{EE (Y2)} = 78.97 + 5.84A + 7.74B - 2.43C - 1.37A B + 1.92AC + 1.75BC \quad \text{---(2)}$$

Equation 2 showed the significant model term, which significantly ($P < 0.05$) affects the VS. A, B, C, AB, AC, and BC are the significant model terms ($p < 0.05$). The second-order model is the best fit for entrapment efficiency because it has a higher R^2 (0.9981) than another experimental model. The predicted R^2 of 0.9904 is in reasonable agreement with the "adjusted R^2 of 0.9948. A model F-value of 382.11 implies that terms with $p < 0.05$ are considered significant. The adequate precision is 61.36, indicating a satisfactory signal. The ANOVA of the fitted model was calculated, and the data are depicted in Table 2. The 3D plot of entrapment efficiency determined the effect of SL, CL, and sonication time (Figure 2) on entrapment efficiency. The entrapment efficiency of all ES formulations was found to be $63.64 \pm 1.43\%$ (TZ-ES1) to $91.52 \pm 2.12\%$ (TZ-ES4). The SL and CL concentrations increase the entrapment efficiency of TZ in the ES. On increasing the SL concentration, the viscosity of the lipid dispersion increases because it increases the hydrophobicity due to the longer acyl length chain and averts the leaching of TZ from the lipid bilayer [29]. It was observed that CL deposited between the free spaces of lipids in bilayers, which lowers the liveness, reduces the drug mobility and diffusion for TZ from ES, and increases the EE of TZ in TZ-ES [30]. The optimized ES was detected from point prediction of the box-bhekhen design software and desirability function. The TZ-ES13 was selected as the best formulation because it has optimum particle size, entrapment efficiency, and a desirable function value. The TZ-ES 13 has 2.25% SL, 3.0% CL, and a 4-minute sonication time. The predicted values of the particle size and entrapment efficiency of TZ-ES13 are 167.53nm and 78.97%, respectively. The experimental value of the TZ-ES13 has 168.0 ± 3.62 nm of particle size and $79.94 \pm 1.43\%$ EE. The prediction errors are very low, i.e., -0.28% for particle size and -1.22% for EE. The size of the particle directly influences the permeation of the formulation through the biological membrane (skin, intestine, etc.). The particle size of all TZ-BES formulations is 73.23 ± 4.62 (TZ-BES1) to $279.62 \pm 5.21\%$ (TZ-BES4) (Table 1). The optimized formulation (TZ-BES13) has a particle size of 168.0 ± 3.62 nm and a PDI of 0.367 (Figure 3A). The PDI value is < 0.5 , indicating ES is uniform in size and has a narrow size distribution. The ZP represents the degree of vesicular system stability because of the repulsive force between charged particles. A greater ZP value indicated that the particle has a low ability to aggregate. The optimized formulation (TZ-BES13) has a ZP of -30 mV (Figure 3B). The ZP of the optimized TZ-BES13 demonstrates the stability of the

colloidal BES formulation. TEM analysis was employed to achieve the desired morphology and size of the optimized TZ-BES13. The TEM micrograph of the optimized formulation (TZ-BES13) was found to be spherical vesicles (Figure 3C).

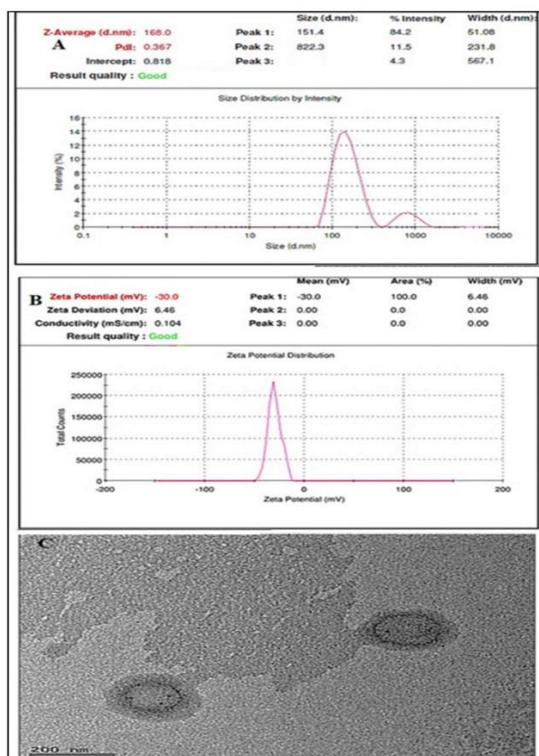


Figure 3: Vesicle size graph and PDI (A), zeta potential (B), and TEM photograph of the optimized TZ-BES13 formulation (C).

The inclusion of ethanol contributes to a smaller ES, while the presence of phospholipids contributes to forming a layer enveloped around the drug molecule. It demonstrated nanovesicular properties, which may facilitate its penetration through the epidermis. The EE of the drug in formulation directly affects the reaching of the desired concentration at the site of action. The EE of all TZ-ES formulations was analyzed and found to be $63.64 \pm 1.43\%$ (TZ-ES1) to $91.52 \pm 2.12\%$ (TZ-ES4) (Table 1). The optimized formulation (TZ-ES13) has an EE of $79.94 \pm 1.43\%$. The drug loading of the optimized formulation (TZ-ES13) is 8.34%. The FTIR spectra of TZ and the optimized formulation TZ-ES13 were analyzed by the KBr pellet method. The FTIR spectrum of TZ shows characteristic stretching vibration peaks of O-H, C \equiv C, and C=C groups at 3483.78 cm^{-1} , 2981.41 cm^{-1} , and 1640.16 cm^{-1} . It also shows the presence of C-O and CH₂ asymmetric vibrations at 1153.43 and 1379.82 cm^{-1} (Figure 4A). The FTIR spectra of the optimized TZ-ES13 showed the characteristic peaks of OH, C \equiv C, C=C aromatic, and C-O at 3635.16 cm^{-1} , 2932.23 cm^{-1} , 1688.09 cm^{-1} , and 1233.25 cm^{-1} respectively (Figure 4B).

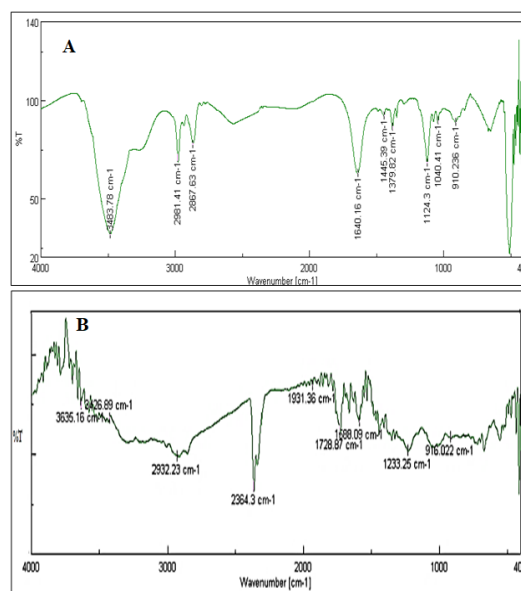


Figure 4: FTIR spectra of (A) pure TZ, (B) optimized TZ-ES13.

The presence of the characteristic peaks in the formulation indicates that there is no interaction between TZ and ingredients. The thermogram of the pure TZ and optimized formulation (TZ-BES13) was analyzed and shown in Figure 5.

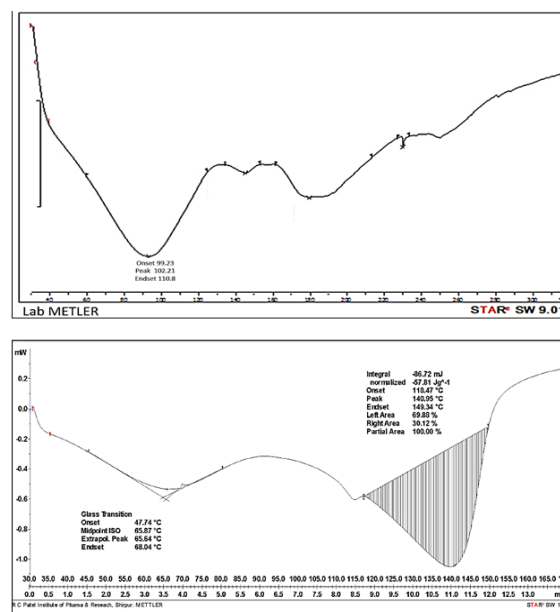


Figure 5: DSC thermogram of (A) pure TZ and (B) optimized TZ-ES13.

The thermogram of TZ shows the characteristic endothermic peak at $102 \text{ }^\circ\text{C}$ (Figure 5A), which corresponds to the melting point of TZ. There is no endothermic peak observed at $102 \text{ }^\circ\text{C}$ of TZ; only broad peaks were observed for the ingredients (Figure 5B). It indicated that TZ was encapsulated in the ethosome matrix. A similar type of finding was found in paeonol-encapsulated ES [31]. The TZ-BES gel was successfully prepared by dispersing the optimized TZ-BES13 into various concentrations of carbopol polymer, as shown in Table 3.

Table 3: composition of different TZ-BES incorporated in carbopol 934P gel

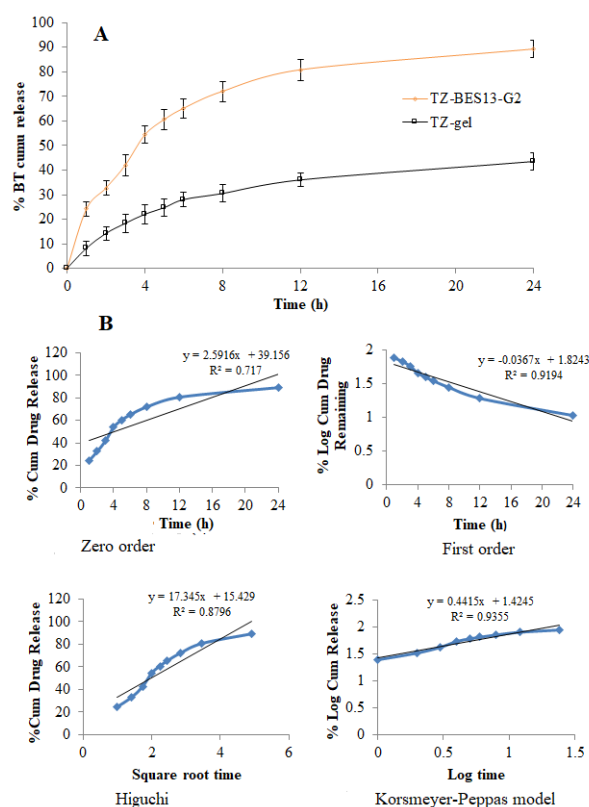
Composition	TZ-ES13-G1	TZ-ES13-G2	TZ-ES13-G3
TZ-ES13 (% w/w)	0.1	0.1	0.1
Carbopol 934 P (% w/w)	2	3	4
Propylene Glycol (% w/w)	5	5	5
Sodium methyl hydroxybenzoate (% w/w)	0.2	0.2	0.2
Purified water	Q.S to 100	Q.S to 100	Q.S to 100

For TDDS, it is necessary to determine the TZ-BES gel's viscosity since it is a prerequisite for the gel's ability to adhere to the skin. All of the produced TZ-BES gel's apparent viscosity was measured, and the results are shown in Table 4. The order of the viscosity of the formulation is TZ-BES13-G1 < TZ-BES13-G2 < TZ-BES13-G3. It was observed that as the concentration of polymer increases, the viscosity increases. The result agreed with the previously published report [5]. Table 4 shows the pH values for all TZ-BES gel samples. All of the TZ-BES gel's pH values fell within the range for skin. Therefore, the formulation is skin-friendly. Layer development on the skin following application and therapeutic action are both greatly impacted by the formulation's spreadability. The result of the spreadability of all developed TZ-BES gel formulations was in the range of $6.91 \pm 0.52 \text{ cm}^2$ (TZ-BES13-G3) to $8.16 \pm 0.23 \text{ cm}^2$ (TZ-BES13-G1) in Table 4. The spreadability falls as the polymer concentration rises. The TZ-BES13-G2 formulation, which has the optimal viscosity and spreadability for the medication content, was chosen as the optimized formulation. In-vitro drug release of TZ-gel and an optimized TZ-BES13-G2 formulation was done using the dialysis bag.

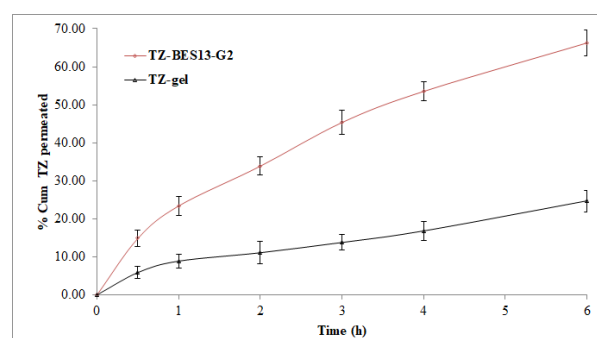
Table 4: The result of characterization parameters of gel

Formulation code	Viscosity (cps)	pH	Drug content (%)	Spreadability (Cm ²)
TZ-BES13-G1	16432±54	6.3±0.3	99.64±0.97	8.2±0.2
TZ-BES13-G2	17235±38	6.5±0.3	99.82±1.0	7.8±0.4
TZ-BES13-G3	19034±43	6.6±0.2	99.89±0.5	6.9±0.5

Figure 6A, which represents the released study's conclusion, Graphically, the TZ-BES13-G2 displayed a TZ release of $24.21 \pm 2.84\%$ in 1 hour and $89.22 \pm 3.52\%$ in 24 hours, respectively. TZ-gel, on the other hand, demonstrated TZ release of $8.23 \pm 2.92\%$ in 1h and $43.54 \pm 3.37\%$ in 24. Low solubility is the cause of the minimal release of TZ from the TZ gel. Due to its improved solubility in ES and nanosize, TZ-BES13-G2 showed a substantial ($p < 0.05$) high TZ release that was sustained by the presence of carbopol gel (32). The result of the kinetic model has been expressed in Figure 6B.

**Figure 6.** shows the in-vitro drug release of TZ from TZ-BES13-G2 (A) and different kinetic model graphs of TZ-BES13-G2 (B).

The Korsmeyer-Peppas model is the best-fitted model because it has the highest R² (0.9335). The value of the release exponent is 0.44 ($P < 0.05$), representing the Fickian diffusion release mechanism [33]. The ex-vivo permeation study of TZ-gel and optimized TZ-BES13-G2 was performed using excised rat skin. The study was performed in a Franz diffusion cell, and the result is shown in Figure 7.

**Figure 7:** Permeation data of TZ from TZ-gel and optimized TZ-BES13-G2 using isolated rat skin. Data were expressed as mean±SD; n: 3.

The % TZ permeation from TZ-gel and optimized TZ-BES13-G2 was found to be $24.67 \pm 2.85\%$ ($493.44 \pm 57.01 \mu\text{g}$) and $66.22 \pm 3.31\%$ ($1324.48 \pm 66.65 \mu\text{g}$), respectively. The fluxes of TZ-gel and optimized TZ-BES13-G2 are $6.52 \mu\text{g}/\text{cm}^2 \cdot \text{hr}$ and $17.52 \mu\text{g}/\text{cm}^2 \cdot \text{hr}$, respectively. The permeability coefficients of the TZ-gel and optimized TZ-BES13-G2 are 8.76×10^{-3} and $3.26 \times 10^{-3} \mu\text{g}/\text{hr}$, respectively. When

compared to plain TZ-gel, the ER of TZ-BES13-G2 is 2.68 times higher. Because of the inclusion of ethanol, SL, and CL, as well as longer skin contact times, TZ-BES13-G2 has a high rate of penetration. It enhanced the penetration of TZ by enhancing the flexibility of ES and by agitating skin lipids. Thus, a large amount of BES penetrated the skin's deeper layer and released TZ [34]. The skin deposition study of TZ-gel and optimized TZ-BES13-G2 was done using excised rat skin for 12 hours. The skin deposition of TZ from TZ-gel and optimized TZ-BES13-G2 was found to be 6.04% and 15.35%, respectively. TZ-BES gel exhibited higher retention than plain TZ-gel because of the presence of penetration enhancers, i.e., ethanol, SL, and cholesterol. Another factor of penetration may take place by the skin via polar, nonpolar, or polar/nonpolar routes. The TZ is lipophilic and may be penetrated by a non-polar pathway [35]. However, TZ-BES13-G2 performs superior to plain gel in

permeation and deposition experiments: the permeability and rigidity of BES as a carrier with a small vesicular size of < 200 nm enhance TZ propagation and integration into the deeper tissue layers, contributing to its accumulation there because they act as a reservoir permitting cumulative drug administration by the coupling of the biocompatible and biodegradable in the BES with the epidermal layer of phospholipids [36]. The stability study of the optimized TZ-BES13-G2 was evaluated at 4 °C, 25 °C/65% RH, and 30 °C/75% RH for three months, and results are depicted in Table 5. The TZ-BES gel exhibited no changes in physical characteristics under this condition. It was also observed that there is no significance ($p>0.05$) in pH, viscosity, or drug content in the TZ-BES13-G2 formulation each time. It concluded that the formulation was stable under the specified conditions.

Table 5: Stability study result of TZ-BES13- gel at different storage conditions

Tests	Initial	Conditions	Time (Month)		
			1 M	2 M	3 M
Physical appearance	Brown, odorless translucent gel	2 to 8 °C	NC	NC	NC
		25 °C/60% RH	NC	NC	NC
		30 °C/75% RH	NC	NC	NC
pH	6.73±0.25 6.50±0.30	4 °C	6.6±0.14	6.6±0.18	6.7±0.24
		25 °C/60% RH	6.51±0.09	6.55±0.17	6.60±0.14
		30 °C/75% RH	6.52±0.21	6.62±0.25	6.64±0.08
Viscosity (cps)	13624 ±10 17235 ±38	4 °C	17236±24	17254±16	17283±31
		25 °C/60% RH	17245±18	17224±22	17221±29
		30 °C/75% RH	17205±33	17282±38	172±26
Drug content (%)	99.82±1.04	4 °C	99.79±1.21	99.73±1.05	99.74±1.04
		25 °C/60% RH	99.80±1.38	99.78±1.65	99.74±1.25
		30 °C/75% RH	99.72±0.84	99.54±1.62	99.45±1.23

NC= No changes

Conclusion

Experimental design software prepared and optimized the binary ethosomes of TZ successfully. The TZ-BES exhibited nanosize vesicles and high drug entrapment efficiency. The TZ-BES gel was prepared using a carbopol gelling agent. The BES-gel showed significantly higher and more sustained releases of TZ than the plain TZ-gel. An ex vivo skin permeation study revealed that TZ-BES-gel has significantly higher permeation and disposition than plain TZ-gel. The finding concluded that BES could be an alternative to improve permeation through skin and stability.

Conflict of interests

No conflict of interest was declared by the authors

Funding source

The authors did not receive any source of fund.

Data sharing statement

Supplementary data can be shared with the corresponding author upon reasonable request.

REFERENCES

- Ahmed B, Qadir MI, Ghafoor S. Malignant melanoma: Skin cancer-diagnosis, prevention, and treatment. *Crit Rev Eukaryot Gene Expr.* 2020;30(4):291-297. doi: 10.1615/CritRevEukaryotGeneExpr.2020028454.
- Ścieżyńska A, Sobiepanek A, Kowalska PD, Soszyńska M, Łuszczynski K, Grzywa TM, et al. A novel and effective method for human primary skin melanocytes and metastatic melanoma cell isolation. *Cancers.* 2021;13(24):6244. doi: 10.3390/cancers13246244.
- Han G, Wu JJ, Del Rosso JQ. Use of topical tazarotene for the treatment of acne vulgaris in pregnancy: a literature review. *J Clin Aesthet Dermatol.* 2020;13(9):E59. PMID: 33133344.
- Wu CS, Chen GS, Lin PY, Pan IH, Wang ST, Lin SH, et al. Tazarotene induces apoptosis in human basal cell carcinoma via activation of caspase-8/t-Bid and the reactive oxygen species-dependent mitochondrial pathway. *DNA Cell Biol.* 2014;33(10):652-666. doi: 10.1089/dna.2014.2366.
- Aggarwal G. Topical nano drug delivery for treatment of psoriasis: Progressive and novel delivery. *Asian J Pharmaceutics.* 2018;12(03): 12(3):S835-S848.
- Kumar N, Goindi S. Development, characterization and preclinical evaluation of nanosized liposomes of itraconazole for topical application: 32 full factorial design to estimate the relationship between formulation components. *J Drug Deliv Sci Technol.* 2021;66:102785. doi: 10.1016/j.jddst.2021.102785.
- El-Enin ASMA, Khalifa MKA, Dawaba AM, Dawaba HM. Proniosomal gel-mediated topical delivery of fluconazole: Development, in vitro characterization, and microbiological evaluation. *J Adv Pharm Technol Res.* 2019;10(1):20. doi: 10.4103/japtr.JAPTR_332_18.

8. Garg AK, Maddiboyina B, Alqarni MHS, Alam A, Aldawsari HM, Rawat P, et al. Solubility enhancement, formulation development and antifungal activity of luliconazole niosomal gel-based system. *J Biomater Sci Polym Ed.* 2021;32(8):1009-23. doi: 10.1080/09205063.2021.1892471.
9. Nemr AA, El-Mahrouk GM, Badie HA. Development and evaluation of proniosomes to enhance the transdermal delivery of cilostazole and to ensure the safety of its application. *Drug Dev Ind Pharm.* 2021;47(3):403-415. doi: 10.1080/03639045.2021.1890111.
10. Hajare A, Dol H, Patil K. Design and development of terbinafine hydrochloride ethosomal gel for enhancement of transdermal delivery: In vitro, in vivo, molecular docking, and stability study. *J Drug Deliv Sci Technol.* 2021;61:102280. doi: 10.1016/j.jddst.2020.102280.
11. Balata GF, Faisal MM, Elghamry HA, Sabry SA. Preparation and characterization of ivabradine HCl transfersomes for enhanced transdermal delivery. *J Drug Deliv Sci Technol.* 2020;60:101921. doi: 10.1016/j.jddst.2020.101921.
12. Jafari A, Daneshamouz S, Ghasemiyeh P, Mohammadi-Samani S. Ethosomes as dermal/transdermal drug delivery systems: applications, preparation and characterization. *J Liposome Res.* 2023;33(1):34-52. doi: 10.1080/08982104.2022.2085742.
13. Nainwal N, Jawla S, Singh R, Saharan VA. Transdermal applications of ethosomes—a detailed review. *J Liposome Res.* 2019;29(2):103-113. doi: 10.1080/08982104.2018.1517160.
14. Abdulbaqi IM, Darwis Y, Khan NA, Assi RA, Khan AA. Ethosomal nanocarriers: the impact of constituents and formulation techniques on ethosomal properties, in vivo studies, and clinical trials. *Int J Nanomedicine.* 2016;11:2279-2304. doi: 10.2147/IJN.S105016.
15. Moolakkadath T, Aqil M, Ahad A, Imam SS, Praveen A, Sultana Y, et al. Fisetin loaded binary ethosomes for management of skin cancer by dermal application on UV exposed mice. *Int J Pharm.* 2019;560:78-91. doi: 10.1016/j.ijpharm.2019.01.067.
16. Jeong WY, Kwon M, Choi HE, Kim KS. Recent advances in transdermal drug delivery systems: A review. *Biomater Res.* 2021;25:1-15. doi: 10.1186/s40824-021-00226-6.
17. Shukla R, Tiwari G, Tiwari R, Rai AK. Formulation and evaluation of the topical ethosomal gel of melatonin to prevent UV radiation. *J Cosmet Dermatol.* 2020;19(8):2093-2104. doi: 10.1111/jocd.13251.
18. Ferrara F, Benedusi M, Sguizzato M, Cortesi R, Baldisserotto A, Buzzi R, et al. Ethosomes and transethosomes as cutaneous delivery systems for quercetin: A preliminary study on melanoma cells. *Pharmaceutics.* 2022;14(5):1038. doi: 10.3390/pharmaceutics14051038.
19. Arora D, Nanda S. Quality by design driven development of resveratrol loaded ethosomal hydrogel for improved dermatological benefits via enhanced skin permeation and retention. *Int J Pharm.* 2019;567:118448. doi: 10.1016/j.ijpharm.2019.118448.
20. Dahash RA, Rajab NA, Almajidi YQ. Investigation of the effect of variable components on the preparation and in-vitro evaluation of lacidipine as an oral nanoemulsion dosage form. *Int J Drug Deliv Technol.* 2021;11(3):1031-1036.
21. Almajidi YQ, Maraie NK, Raauf AM. Utilization of solid in oil nanodispersion to prepare a topical vemurafenib as potential delivery system for skin melanoma. *Appl Nanosci.* 2023;13(4):2845-2856. doi: 10.1007/s13204-021-02158-y.
22. Almajidi YQ, Maraie NK, Raauf AM. Modified solid in oil nanodispersion containing vemurafenib-lipid complex-in vitro/in vivo study. *F1000Res.* 2022;11:841. doi: 10.12688/f1000research.
23. Muslim RK, Maraie NK. Preparation and evaluation of nano-binary ethosomal dispersion for flufenamic acid. *MaterialsToday: Proceedings.* 2022;57:354-361. doi: 10.1016/j.matpr.2021.09.239.
24. Fathalla D, Youssef EM, Soliman GM. Liposomal and ethosomal gels for the topical delivery of anthralin: preparation, comparative evaluation and clinical assessment in psoriatic patients. *Pharmaceutics.* 2020;12(5):446. doi: 10.3390/pharmaceutics12050446.
25. Maraie NK, Almajidi YQ. Effect of different mucoadhesive polymers on release of ondansetron HCl from intranasal mucoadhesive in situ gel. *Al Mustansiriyah J Pharm Sci.* 2017;17(2):10. doi: 10.32947/ajps.v17i2.47.
26. Maraie NK, Almajidi YQ. Application of nanoemulsion technology for preparation and evaluation of intranasal mucoadhesive nano-in-situ gel for ondansetron HCl. *J Glob Pharma Technol.* 2018;10(03):431-442.
27. Rapalli VK, Singhvi G, Srividya G, Waghule T, Dubey S, Saha R, et al. Stability indicating liquid chromatographic method for simultaneous quantification of betamethasone valerate and tazarotene in in-vitro and ex-vivo studies of complex nanoformulation. *J Sep Sci.* 2019;42:3413-3420. doi: 10.1002/jssc.201900538.
28. Chen J-G, Liu Y-F, Gao T-W. Preparation and anti-inflammatory activity of triptolide ethosomes in an erythema model. *J Liposome Res.* 2010;20(4):297-303. doi: 10.3109/08982100903544144.
29. Maritim S, Boulas P, Lin Y. Comprehensive analysis of liposome formulation parameters and their influence on encapsulation, stability and drug release in glibenclamide liposomes. *Int J Pharm.* 2021;592:120051. doi: 10.1016/j.ijpharm.2020.120051.
30. Rushmi ZT, Akter N, Mow R, Afroz M, Kazi M, Matas M, et al. The impact of formulation attributes and process parameters on black seed oil loaded liposomes and their performance in animal models of analgesia. *Saudi Pharm J.* 2016;25. doi: 10.1016/j.jsps.2016.09.011.
31. Ma H, Guo D, Fan Y, Wang J, Cheng J, Zhang X. Paeonol-loaded ethosomes as transdermal delivery carriers: design, preparation and evaluation. *Molecules.* 2018;23(7):1756. doi: 10.3390/molecules23071756.
32. Alshehri S, Hussain A, Altamimi MA, Ramzan M. In vitro, ex vivo, and in vivo studies of binary ethosomes for transdermal delivery of acyclovir: A comparative assessment. *J Drug Deliv Sci Technol.* 2021;62:102390. doi: 10.1016/j.jddst.2021.102390.
33. Peppas NA. 1. Commentary on an exponential model for the analysis of drug delivery: Original research article: a simple equation for description of solute release: I II. Fickian and non-Fickian release from non-swelling devices in the form of slabs, spheres, cylinders or discs, 1987. *J Control Release.* 2014;190:31-32. PMID: 25356469.
34. Mbah CC, Builders PF, Attama AA. Nanovesicular carriers as alternative drug delivery systems: ethosomes in focus. *Expert Opin Drug Deliv.* 2014;11(1):45-59. doi: 10.1517/17425247.2013.860130.
35. David SRN, Hui MS, Pin CF, Ci FY, Rajabalaya R. Formulation and in vitro evaluation of ethosomes as vesicular carrier for enhanced topical delivery of isotretinoin. *Int J Drug Deliv.* 2013;5(1):28.
36. El-Shenawy AA, Abdelhafez WA, Ismail A, Kassem AA. Formulation and characterization of nanosized ethosomal formulations of antigout model drug (febuxostat) prepared by cold method: In vitro/ex vivo and in vivo assessment. *AAPS PharmSciTech.* 2019;21(1):31. doi: 10.1208/s12249-019-1556-z.